Lawrence Berkeley National Laboratory

Modelling of Non-linear CHP Efficiency Curves in Distributed Energy Systems

Christian Milan[1,2], Michael Stadler[2,3], Gonçalo Cardoso[2,4], Salman Mashayekh[2]

[1]Department of Energy Technology, Aalborg University, Pontoppidanstræde 101, 9220 Aalborg, Denmark

[2]Lawrence Berkeley National Laboratory, 1 Cyclotron Road, Berkeley, CA 94720, USA

[3]Center for Energy and Innovative Technologies (CET), Doberggasse 9, 3681 Hofamt Priel, Austria

[4]Instituto Superior Técnico, University of Lisbon, Avenida Rovisco Pais 1, 1049-001 Lisboa, Portugal

To be published in Applied Energy

March 2015

Disclaimer

1   **Modelling of non-linear CHP efficiency curves in distributed energy systems**
2
3   Christian Milan[a,b], Michael Stadler[b,c*], Gonçalo Cardoso[b,d], Salman Mashayekh[b]
4
5   [a] Department of Energy Technology, Aalborg University, Pontoppidanstræde 101, 9220
6   Aalborg, Denmark
7   [b] Lawrence Berkeley National Laboratory, University of California, 1 Cyclotron Rd,
8   Berkeley, CA, USA
9   [c] Center for Energy and innovative Technologies (CET), Doberggasse 9, 3681 Hofamt Priel,
10 Austria
11 [d] Instituto Superior Técnico, University of Lisbon, Avenida Rovisco Pais 1, 1049-001 Lisboa,
12 Portugal
13

14 **ABSTRACT**

15 Distributed energy resources gain an increased importance in commercial and industrial
16 building design. Combined heat and power (CHP) units are considered as one of the key
17 technologies for cost and emission reduction in buildings. In order to make optimal decisions
18 on investment and operation for these technologies, detailed system models are needed. These
19 models are often formulated as linear programming problems to keep computational costs and
20 complexity in a reasonable range. However, CHP systems involve variations of the efficiency
21 for large nameplate capacity ranges and in case of part load operation, which can be even of
22 non-linear nature. Since considering these characteristics would turn the models into non-
23 linear problems, in most cases only constant efficiencies are assumed. This paper proposes
24 possible solutions to address this issue. For a mixed integer linear programming problem two
25 approaches are formulated using binary and Special-Ordered-Set (SOS) variables. Both
26 suggestions have been implemented into the optimization model DER-CAM to simulate
27 investment decisions of CHP micro-turbines and CHP fuel cells with variable efficiencies.
28 The approaches have further been applied successfully in a case study with four different
29 commercial buildings. Comparison of the results between the standard version and the new
30 approaches indicate that total annual system costs remain almost unchanged. System
31 performance is subject to change and storage technologies become more important. Part load
32 operation has mainly been found important for fuel cell units. The micro-turbine is found
33 almost exclusively in full load, thus rendering the application of the new approaches for this
34 technology unnecessary for the considered unit sizes and building types. The approach using
35 binary variables was the most promising method to model variable efficiencies in terms of
36 computational costs and results. It should especially be considered for specific fuel cell
37 technologies. Further investigation on the impacts of this approach on the prediction of fuel
38 cell and micro-turbine performance is suggested.
39

42 **Nomenclature**

43 *Subscripts*

44 *Bat*   Electric Vehicle Battery

---

* Corresponding author. Tel.: +1 (510) 486-4929 or +43 (0)664 7390-7185. *E-mail address:* MStadler@lbl.gov or MStadler@cet.or.at (M. Stadler).

45	*DER*	Distributed Energy Resources
46	*DR*	Demand response
47	*el*	electricity
48	*n*	capacity sizes index
49	*inst*	installed
50	*m*	operational load level index
51	*k*	number of units index
52	*M*	number of capacity sizes
53	*N*	number of operational load levels
54	*t*	time index
55	T	number of time steps

56 *Superscripts*

57	^	tabled value

58 *Dependent Variables*

59	α	heat to power ratio
60	*C*	system costs
61	*E*	system emissions
62	*EV*	electric vehicle
63	η	efficiency
64	*F*	fuel consumption
65	*I*	income from energy sales
66	*v*	weighting variable (binary variable)
67	ω	weighting variable (binary variable)
68	*x*	weighting variable (type SOS2)
69	*y*	weighting variable (type SOS1)
70		

71 *Decision Variables*

72	*P*	unit capacity
73	*U*	operational load level
74		

1. Introduction

76 Optimizing building energy supply systems with high temporal resolution over a large
77 timespan – usually one year of hourly time steps – can result in mathematically complex
78 problems with long calculation procedures before reaching optimal solutions. In order to keep
79 computational efforts within reasonable levels several simplifications and assumptions are
80 commonly used. Such simplifications can include those used in linear models that guarantee
81 convergence and optimality, albeit sometimes at the cost of significant adverse impacts on
82 model accuracy [1]. Looking at energy systems models specifically, a common approximation
83 used concerns the efficiency of conventional power generation technologies, which in most
84 cases is treated as a constant. This approximation might be close to reality for some
85 technologies and operating conditions, but a very rough simplification for others. This paper
86 will address this topic by modeling efficiency curves of conventional power generation
87 technologies with different levels of accuracy, as we will discuss later in the paper.
88
89 Using Combined Heat and Power (CHP) for energy supply is very often a sustainable and
90 economic strategy to reduce fuel demand, and CHP technologies are among the most
91 promising solutions for fuel saving, emission reduction, and fossil fuel independency [1]–[3].

92   However, the economic convenience of CHP systems depends on the specific conditions
93   under which they operate, since their performance significantly changes when operating in
94   partial load [1]–[6]. The electrical and thermal efficiencies of CHP units depend on the
95   technology, unit size (capacity), and loading conditions (operating point). M. Bianchi et al. [1]
96   report that the nameplate electric efficiency and thermal efficiency at maximum recovered
97   thermal power can range between 10%-30%, and respectively 40%-90%. Moreover, their
98   electric efficiency in partial loads can degrade more than 20% compared to the full load
99   efficiency. Higher partial load efficiency variations are also reported in [7]. CHP systems
100   have potential to be used in various applications such as residential buildings, hospitals, and
101   supermarkets, where electrical, thermal, and cooling demand is time-variant [1]. Application
102   of CHP technologies in time-varying demand environments along with their partial load
103   efficiency variations signifies the importance of modelling these technologies with load
104   dependent efficiencies.

105
106   To model and analyze the impact of partial load efficiencies for CHP technologies in an
107   optimal DER investment problem, this paper proposes two linear approaches. Both
108   approaches allow for integrating nonlinear efficiency curves into the optimization problem
109   without abandoning the problem linearity. This type of modeling and analysis has not been
110   carried out in the past. To model DER efficiencies (CHP technologies in particular),
111   researchers either use constant efficiencies to simplify their model and keep it linear, or
112   consider nonlinear efficiencies in nonlinear models. While the former approach may result in
113   non-optimal results due to over-simplification, the latter may not be able to find the global
114   optimum solution, may not find a solution at all due to the complexity of the resulting model,
115   or increase the computational costs dramatically.

116
117   Some examples of the models using constant efficiencies for CHP technologies are given in
118   [8]–[16] . Milan et al. [8] propose an investment planning methodology to minimize total
119   costs of 100% DER-based supply systems, considering the interdependencies between
120   different supply technologies, for both Net Zero Energy Buildings (Net ZEB) and Low
121   Energy Buildings (LEB). They formulate the problem as a Mixed Integer Linear Program
122   (MILP). As in most of the similar models, the output from this model suggests optimal sizes
123   of supply technologies and/or building load reduction measures, and proposed operational
124   schedules. To simplify the model, constant CHP efficiencies are used in this work. Münster et
125   al. [9] analyze the competition between district heating and other types of individual heating,
126   and use also constant efficiencies to perform the analysis. The work in this paper is motivated
127   by the increase in the attractiveness of individual solutions provided by the new technologies
128   such as electric heating, heat pumps, and micro-CHP. In a similar application, Lund et al. [10]
129   study different district and individual heating options for Denmark, and use constant
130   efficiencies for the studies. Liu et al. [11] present a framework for optimal design of energy
131   systems in commercial buildings, which aims to improve energy efficiency and environmental
132   performance. They develop a multi-objective mixed-integer optimization problem to address
133   the two economic and environmental objectives, and use constant efficiencies for all
134   technologies. Similarly, Ren et al. [12] propose a MILP model for the planning and evaluation
135   of DER systems, which delivers the optimal DER technologies to be installed and the optimal
136   operation schedules, given the site's energy loads, weather conditions, tariff structure, and
137   candidate DER technology characteristics. In this model, again only constant efficiencies are
138   considered for all DER technologies, including the ones with heat recovery capabilities.
139   Hawkes et al. [13] develop a linear model for the high level microgrid system design,
140   including generator and storage unit commitment, to minimize the cost. A constant efficiency
141   is considered for the CHP units in this model. In another work in [14], a mixed integer linear

142 programming model is developed for long-term optimization of cogeneration systems, which
143 uses load-independent fixed efficiencies.
144
145 Cho et al. [15] present an optimal energy dispatch algorithm that minimizes the cost of
146 electric and natural gas supplies. This work develops a linear programming model with
147 cooling, heating, and electrical load demand constraints and constraints of Combined Cooling,
148 Heating, and Power (CCHP) components' efficiencies. In this model, the efficiency of each
149 CCHP component is assumed to be constant. Also, in another work in [16], Cho et al. present
150 results from operation optimization of CCHP systems for various climate conditions, which
151 aims to reduce operational costs, primary energy consumption, and carbon dioxide emissions.
152 In this work, they assume a linear behaviour with a constant slope for the electricity output to
153 fuel ratio, thus constant efficiencies. To avoid "on/off" constraints in their MILP model, they
154 use two LP simulations and choose the smallest output value.
155
156 There are also some research works that use non-fixed partial load efficiency models for CHP
157 technologies, but do not keep the problem linear and use nonlinear formulations. Such
158 examples are common in combined heat and power economic dispatch formulations, such as
159 [17]–[23]. For the fuel consumption of a CHP unit in these formulations, convex quadratic
160 functions in both output power and output heat of the unit are used, which result in nonlinear
161 formulations. To solve the resulting nonlinear optimization problems, heuristic methods are
162 commonly applied, e.g. Particle Swarm Optimization (PSO) [17], [18], Teaching Learning
163 Based Optimization (TLBO) [19], Mesh Adaptive Direct Search (MADS) [20], and Cuckoo
164 Search Algorithm [21]. Heuristic optimization methods, especially for large-scale
165 optimization problems, are not guaranteed to find a solution and the solution they find may
166 not be the global solution. Hence in large-scale optimization problems with millions of
167 decision variables, such as the ones discussed in this paper, linear problem formulations are
168 highly preferred over nonlinear ones.
169
170 This paper presents two piecewise linear approximation methods for nonlinear DER
171 efficiency curves. Both suggestions have been implemented in the optimization model DER-
172 CAM (Distributed Energy Resources and Customer Adoption Model), which traditionally
173 used fixed efficiencies for CHP micro-turbine and fuel cell technologies [24]–[26]. DER-
174 CAM is a decision support tool for decentralized energy systems developed by the Lawrence
175 Berkeley National Laboratory (LBNL). It is formulated as a Mixed-Integer Linear Program
176 (MILP), and implemented in the General Algebraic Modeling System (GAMS). DER-CAM
177 has two main versions, i.e. the Investment and Planning DER-CAM, and the Operations
178 DER-CAM. The Investment and Planning DER-CAM picks optimal microgrid/building
179 equipment combinations and sizes, and their corresponding dispatch, using three day types
180 per month to represent a year of historic hourly energy loads, technology costs and
181 performance, fuel prices, historic weather data, and the utility tariff. The Operations DER-
182 CAM is used for microgrid/building dispatch optimization for a given period, typically
183 several days to a week ahead, with a time resolution of 5 minutes, 15 minutes, or 1 hour,
184 using weather and load forecast for the optimization period, and assuming a known
185 technology portfolio [27]. This work uses the Investment and Planning version of DER-CAM.
186
187 The contributions of this paper are twofold. First, to address the problem of including
188 nonlinear efficiencies in DER optimization problems, without sacrificing the problem
189 linearity, this paper proposes two alternative stepwise methods to approximate two-
190 dimensional non-linear DER efficiency curves. In the first method, binary variables are used
191 to approximate nonlinear efficiency curves with piecewise linear ones. In the second method,

192 Special-Ordered-Set (SOS) variables are used to approximate the nonlinear efficiency curves.
193 SOS variables are defined as consecutive, ordered sets of variables, where no more than one
194 or two (based on SOS type) adjacent elements in the ordered set can take non-zero values.
195 The problem formulation resulting from the former method can be solved by any solver
196 capable of solving mixed-integer linear problems. On the contrary, the latter method results in
197 a formulation that can only be solved by solvers recognizing SOS variables. The performance
198 of these two methods is investigated in detail by applying them in a case study consisting of
199 four different buildings. The second contribution of this paper is in analyzing the impact of
200 considering nonlinear DER efficiency curves of three relevant technologies on the final
201 solution and recommending best practices for including such nonlinear efficiency curves for
202 other similar problems.
203
204 The structure of the following parts of the paper is as follows:
205 • Section 2 describes the optimization model DER-CAM which was adapted in this
206 paper.
207 • Section 3 discusses the efficiency characteristics of DER technologies in terms of
208 installed capacity and part load.
209 • Section 4 introduces the theory for two linearization approaches of non-linear
210 efficiency curves.
211 • Section 5 presents the case study performed together with the modifications
212 undertaken in DER-CAM and detailed results.
213 • Section 6 summarizes the main findings of the case study and gives recommendations
214 for further action.
215

216 ## 2. DER-CAM

217 The Distributed Energy Resources Customer Adoption Model (DER-CAM) is a decision
218 support tool developed at Lawrence Berkeley National Laboratory with the purpose of
219 optimizing DER investment and operation decisions in microgrids and building energy supply
220 systems. The model is formulated as a mixed integer linear program (MILP), and being firstly
221 introduced in the year 2000 it has been constantly extended and applied throughout several
222 dozen case studies [28]–[33]. Currently, DER-CAM features two main branches: one to
223 optimize investment decisions based on historic information – Investment & Planning DER-
224 CAM, and a second one to determine optimal operational schedules of installed equipment
225 and for predictive microgrid controller design, based on weather and load forecasts –
226 Operations DER-CAM. Investment & Planning DER-CAM is publicly available through a
227 web-based interface [28] and will be the reference for further discussions on DER-CAM in
228 this work.
229
230 Once detailed load profiles are known, such as demand data for space heating, hot water,
231 cooling, and electricity, DER-CAM determines the optimal installed capacity of DER
232 technologies with respect to a user-defined objective function, generally economic and/or
233 environmental. Key input data also includes electricity and natural gas tariffs, and prices on
234 relevant fuels and financial subsidies, if applicable. For all considered DER technologies,
235 performance models are implemented based on state-of-the-art technical specifications,
236 namely with regards to efficiencies and heat-to-power ratios. Moreover, detailed cost data for
237 investment, operation and maintenance of each DER unit are considered in the model. In
238 order to solve the DER investment problem, DER-CAM determines on an hourly basis the
239 optimal scheduling of the candidate energy supply system for one reference year. Therefore,
240 investment decisions are based on a bottom up approach and results will also include detailed

241 operational schedules for all selected technologies, along with key variables such as total
242 annual energy costs and CO_2 emissions.
243
244 The hourly system performance is based on detailed energy balances. Fig. 1 indicates the
245 energy resources, energy flows and end-uses implemented in DER-CAM in the form of a
246 SANKEY diagram [26]. This provides a full view of energy flows in the form of arrows from
247 possible resources considered within the optimization and how they relate to consumption.
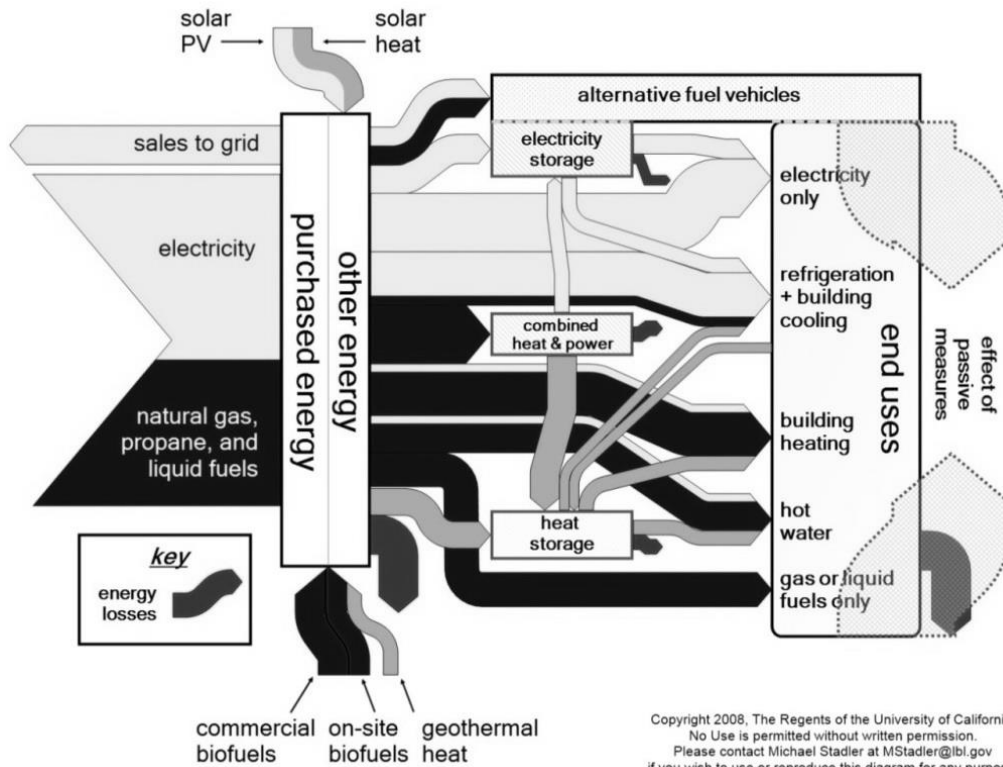
248
249 *Fig. 1. SANKEY diagram indicating energy flows in DER-CAM [26]*

250 Energy sources considered in DER-CAM include utility natural gas, biofuels, solar radiation,
251 utility electricity, and geothermal heat. Dark shaded arrows in Fig. 1 represent natural gas and
252 biofuels. Light grey shaded arrows represent electricity, and the dark grey colour stands for
253 heat and recoverable waste heat. DER-CAM identifies the optimal system configuration in
254 terms of costs and/or environmental impact, while meeting all shown energy demands on the
255 right side of the diagram, defined for each hourly time step in a given site. Similarly to
256 consumption profiles, on-site resource availability such as solar radiation and other boundary
257 conditions can be highly fluctuating, and the energy flows for each carrier might reflect these
258 fluctuations accordingly.
259
260 The key generation options in DER-CAM are CHP technologies, which interconnect supply
261 and storage of electricity and heat, although other options such as photovoltaic and solar
262 thermal panels are available. Recently, DER-CAM has also been extended to consider electric
263 vehicles for vehicle-to-building services [34], and several other features are currently under
264 development.
265
266 DER-CAM allows a flexible objective function definition, such as minimizing total annual
267 energy costs, CO_2 emissions, net energy minimization, or combinations of them. Eq. 1 defines
268 the objective function for cost optimization:
269

270 $$min\, f_{costs}(P_{inst}, U_t) = C_{total} = C_{el} + C_{DER} + C_{fuel} + C_{DR} + C_{Bat} - I \qquad (1)$$

271

272 The total annual energy costs C_{total} depend on the installed capacity of DER technologies,
273 P_{inst}, and their operational level U_t at each hour t. These variables have impacts on the
274 electricity costs C_{el}, on the amortized installation and maintenance costs of DER components
275 C_{DER}, on fuel costs C_{fuel}, on costs of adopting demand response measures C_{DR}, and also on
276 electric vehicle battery degradation costs due to interactions with the building energy supply
277 system C_{Bat}, although electric vehicles are not considered in this work. Moreover, income
278 generated by energy sales to public networks I is subtracted from the total costs.

279

280 The objective function for the minimization of CO_2 emissions is formulated according to Eq.
281 2:

282

283 $$min\, f_{CO2}(P_{inst},\, U_t) = E_{CO2,total} = E_{CO2,el} + E_{CO2,fuel} + E_{CO2,EV} \qquad (2)$$

284

285 Similarly to annual energy costs, the total annual CO_2 emissions $E_{CO2,\,total}$ are a function of
286 installed DER capacity and operational schedules. They are defined in DER-CAM as the sum
287 of CO_2 emissions related to the generation of grid-supplied electricity, emissions caused by
288 onsite fuel consumption $E_{CO2,fuel}$, and CO_2 emissions caused by electric vehicle charging $E_{CO2,}$
289 $_{EV}$ (not considered in this work).

290 Schematically, the formulation implemented in DER-CAM can be described according to Fig.
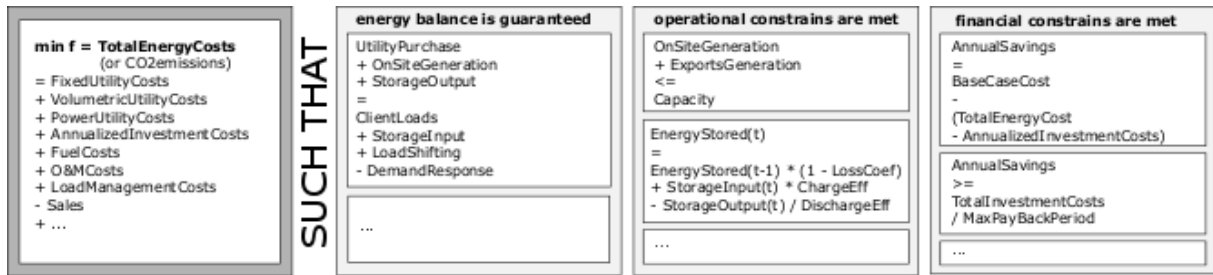291 2.

292

293 *Fig. 2. Schematic representation of DER-CAM*

294 Several assumptions and simplifications are applied in DER-CAM to model technology
295 performance and customer decisions. It is estimated that the customer bases his investment
296 and operation strategy solely on optimizing the direct economic benefit, CO_2 reductions, or a
297 combination of both. Concerning the technologies, constant efficiencies are assumed for the
298 operation throughout the whole component lifetime without considering possible output
299 declines. Furthermore, start-up and ramping restrictions of supply units are not considered, as
300 well as reliabilities and power quality benefits.

301

302 Researching the impact of assuming constant efficiencies for supply components is the
303 objective of this work. In the following chapters relevant technologies will be identified and
304 two approaches are described to address this issue. Furthermore, the extension of the
305 Investment & Planning version of DER-CAM is presented in order to implement these
306 approaches.

307

308 **3. Efficiencies of DER-Technologies**

309 Typically, it can be stated that the maximal electrical efficiency $\eta_{el,max}$ of DER technologies
310 depends on two key factors: the installed unit capacity P_{inst}, and the operating load level at a
311 given time U_t:
312

313 $$\eta_{el} = f(P_{inst,}U_{t)} \tag{3}$$

314

315 In Fig. 3, the maximal electrical efficiency of natural gas powered Internal Combustion
316 Engines (ICE) is shown for different unit sizes. This relation is based on data from [35],
317 which gathered and analysed data from several hundred market available units of different
318 sizes in Germany. The figure illustrates significantly lower efficiencies for small capacities
319 and a non-linear relationship in the depicted range between the installed electrical power and
320 the maximal efficiency.
321
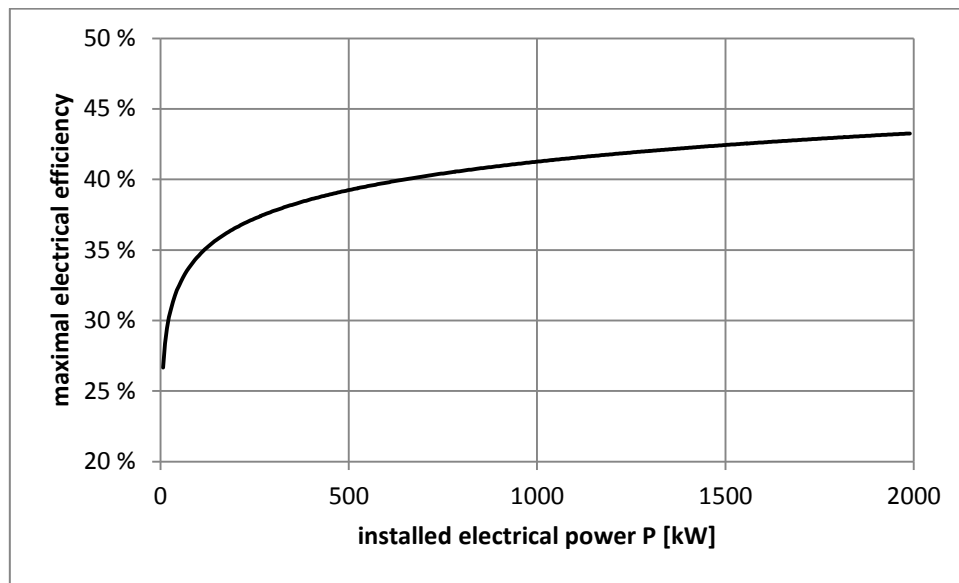
322
323 *Fig. 3. Maximal electrical efficiencies for natural gas powered ICEs [35]*

324 It should be noted that the graph in Fig. 3 is heavily dependent on the fuel and only valid for
325 natural gas powered plans. For other fuels, e.g. diesel, different characteristics may apply and
326 the relation between installed power and maximum electrical efficiency can be close to linear
327 behaviour for certain fuel types [35].
328
329 Besides the installed capacity, the operational load level U_t also influences the efficiency of
330 certain technologies. Fig. 4 depicts the part load performance of a typical natural gas powered
331 ICE based on data given in [36]. As in Fig. 3, a non-linear correlation can be observed.
332

333
334 *Fig. 4. Electrical efficiencies for a typical natural gas powered ICE in part load [36]*

335 Based on these observations, considering variable efficiencies results in a two-dimensional
336 non-linear problem when selecting the optimal unit sizes to meet energy demand in a given
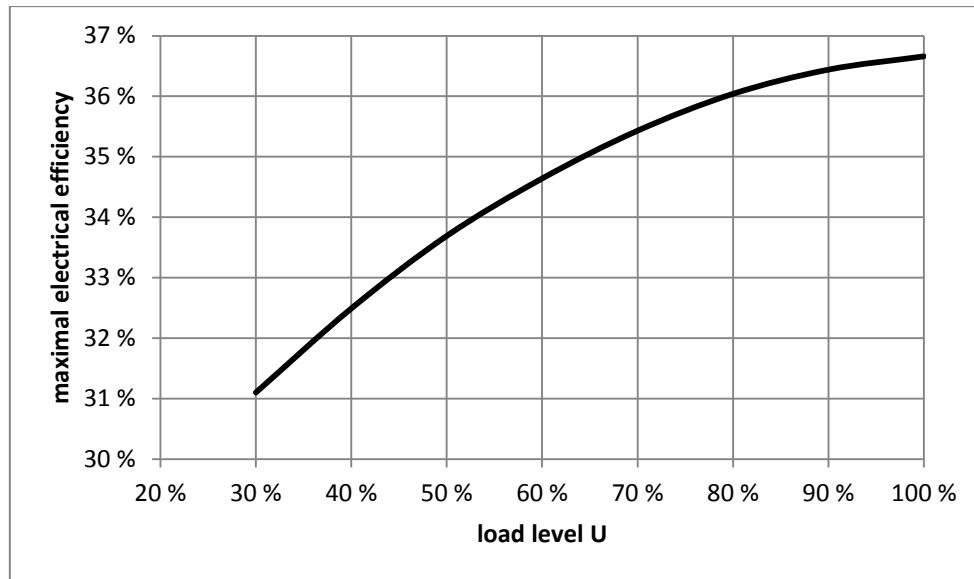337 building or microgrid, although this dependency is not valid for all technologies.
338
339 Table 1 lists relevant supply technologies considered in DER-CAM, indicating whether or not
340 they exhibit considerable efficiency variations during part load operation, and if they were
341 considered in the developments introduced by this work.
342
343 From the seven technologies listed, all combustion technologies and fuel cells have part load
344 characteristics. The maximal efficiencies of photovoltaic panels (PV), solar thermal collectors
345 (ST), and heat pumps (HP) do not differ significantly on part load conditions or on installed
346 capacity.
347
348
349 Table 1. Relevant technologies in DER-CAM with part-load classification
350

Technology	Variable part load efficiency	Included in this work
Photovoltaic	no	-
Solar Thermal Collector	no	-
Heat Pump	no	-
Fuel Cell (FC)	yes	yes
Internal Combustion Engine (ICE)	yes	yes
Micro-turbine (MT)	yes	yes
Gas Turbine	yes	no

351
352 The developments introduced in this work regarding variable efficiencies focus on Fuel Cells
353 (FC), Internal Combustion Engines (ICE) and Micro-turbines (MT), as Gas Turbines are
354 typically available in large capacity sizes and are not the focus of this work.
355

4. Modelling two-dimensional non-linear efficiency curves

Since efficiencies are directly dependent on the installed capacity P_{inst} and operational load level U_t, both parameters can be identified as the decision variables defining the energy conversion capability of a unit over time. P_{inst} and U_t influence the conversion efficiency, the fuel consumption F_t and, if connected to a heat exchanger in a CHP system, the heat output $P_{heat,t}$. Since the load level U_t can change for each point in time, the functions are dependent on the time index t as shown in Eqs. 4 to 6, where P_{inst} and U_t refer to the electrical output in all equations:

$$P_{el,t} = P_{inst} \cdot U_t \tag{4}$$

$$F_t = \frac{(P_{inst} \cdot U_t)}{\eta_{el,t}} \tag{5}$$

$$P_{heat,t} = P_{inst} \cdot U_t \cdot \alpha_t \tag{6}$$

with α_t being the heat to power ratio defined as in Eq. 7:

$$\alpha_t = \frac{\eta_{heat,t}}{\eta_{el,t}} \tag{7}$$

and $\eta_{el,t}$ being a function of P_{inst} and U_t.

Even though the efficiency curves shown in Fig. 3 and 4 can be linearized using the approaches presented later in this paper, one should be aware of that all three variables $P_{el,t}$, F_t and $P_{heat,t}$ are dependent on the product of P_{inst} and U_t. Their calculation after the determination of these two decision variables would create an additional non-linear problem. For this reason all values for $P_{el,t}$, F_t and $P_{heat,t}$ are calculated beforehand for the range of possible installed capacities and operational load levels. Table 2 shows electrical efficiencies of a natural gas powered ICE for two installed capacities and several load levels. The values are based on data given in [36].

Table 2. Electrical efficiencies of natural gas powered ICE [36]

Installed capacity option, $P_{inst,n}$		Load level, $U_{m,t}$								
		$U_{1,t}$ 0%	$U_{2,t}$ 30%	$U_{3,t}$ 40%	$U_{4,t}$ 50%	$U_{5,t}$ 60%	$U_{6,t}$ 70%	$U_{7,t}$ 80%	$U_{8,t}$ 90%	$U_{9,t}$ 100%
$P_{inst,1}$	60 kW	0	0.246	0.257	0.267	0.274	0.28	0.285	0.288	0.29
$P_{inst,2}$	250 kW	0	0.255	0.266	0.276	0.283	0.29	0.295	0.298	0.30

From now on tabled values will be marked with a circumflex (^) and the indices $_n$ and $_m$ will refer to elements in the set of the discrete installed capacity options and to considered load levels, respectively. The tables for $P_{el,t}$, F_t and $P_{heat,t}$ form the basis for two approaches, which allow linearizing and approximating two-dimensional non-linear efficiency curves into MILPs. Both approaches will be elaborated in the following sections.

395 **4.1. Approach 1 - Linearization using binary variables**

396 The first approach is based on binary variables, which are used to form classes with each class
397 containing a certain tabled value. Fig. 5 shows the principle equations and their relationship
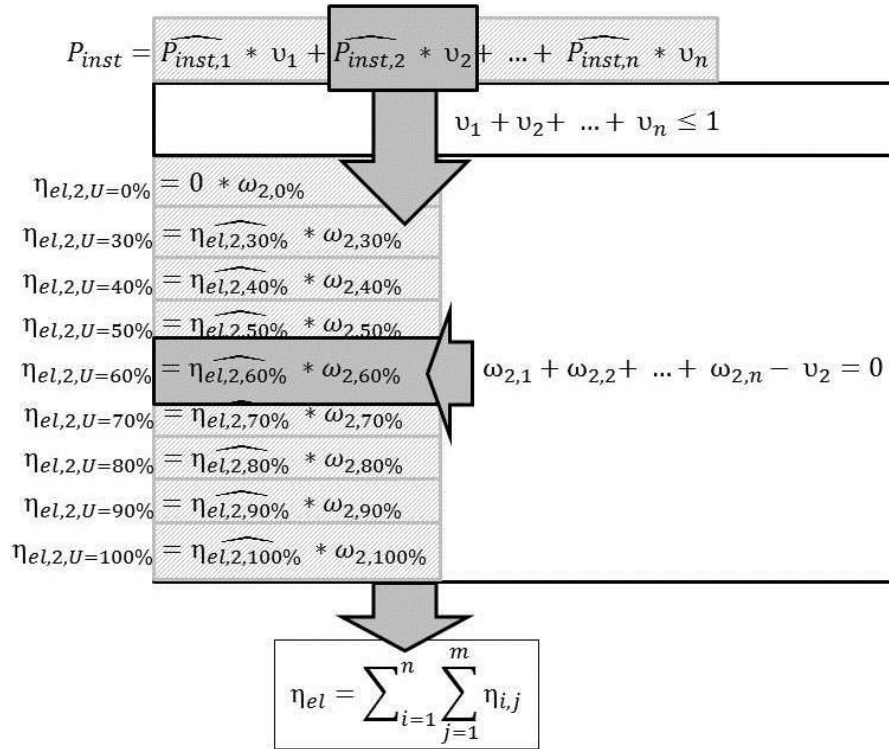398 for the binary approach.

399

400
401 *Fig. 5. Schematic of the binary approach choosing efficiencies based on installed capacity*
402 *and operational load level at each time step t*

403 The decision on the installed capacity is guaranteed by Eq. 8, which consists on the
404 summation over the product of tabled capacities options $P_{inst,n}$ with a corresponding binary
405 variable for each option:

406

407 $$P_{inst} = \sum_n (P_{inst,n}^{\wedge} \cdot v_n) \tag{8}$$

408

409 The index n refers to the nameplate capacity specified beforehand in the data table with N
410 indicating the number of tabled sizes.
411 In order to assure that only one capacity is chosen, the constraint in Eq. 9 is introduced. Also,
412 it should be noted that since the investment decision is not time-dependent, these equations
413 hold for the entire calculation process.

414

415 $$\sum_n v_n \leq 1 \tag{9}$$

416

417 The operational level of the installed capacity option n in each time step t is determined by
418 Eq. 10, where the binary variable v_n guarantees the lookup is made on the appropriate
419 capacity option, and the binary variable $\omega_{n,m,t}$ guarantees that only one operating point is
420 selected in each time step:

421

422 $$\sum_m \omega_{n,m,t} - v_n = 0 \text{ for n=\{1,2,...,N\} and t=\{1,2,...,T\}} \tag{10}$$

423

424 Thus, solving Eq. 10 over time determines the operation point m,t for installed capacity option
425 n, for which efficiency, fuel consumption, and power output can be determined based on the
426 tabled values, as shown below for electric efficiency:
427
428 $$\eta_{el,n,m,t} = \eta^{\wedge}_{el,n,m} \cdot \omega_{n,m,t} \text{ for n=\{1,2,…,N\}, m=\{1,2,…,M\} and t=\{1,2,…,T\}} \qquad (11)$$
429
430 In total, Eq. 11 involves n by m and t calculations. Thus, the final values used to extend the
431 existing DER-CAM formulation in a seamless way are obtained by summation, where all
432 binary variables except the selected n,m pair are null for each time step t, as shown in Eq. 12:
433
434 $$\eta_{el,t} = \sum_n \sum_m \eta_{el,n,m,t} \text{ for t=\{1,2,…,T\}} \qquad (12)$$
435
436 While only the electric efficiency is mentioned, the corresponding fuel consumption,
437 electricity output and, if relevant, heat generation are calculated in a similar fashion according
438 to Eq. 10 and 11 using the same binary variables $\omega_{n,m,t}$.
439
440 While the use of binary variables for step-wise approximations of non-linear functions is not
441 new, this technique has not been previously used in DER investment problems. It provides an
442 effective way to increase the accuracy of DER modeling, but it must also be pointed out that
443 this formulation carries the disadvantage only allowing single tabled values to be selected,
444 with no interpolation between them. This decreases the precision of the results and for very
445 restricted energy systems, such as buildings in islanded mode, there might be no feasible
446 solution. Furthermore, the flexibility of the methodology is considerably reduced, as
447 capacities have to be pre-defined in the data tables. Thus, if the user intends to investigate unit
448 sizes outside of the table range, the relevant data has to be gathered prior to model
449 application.
450

451 **4.2. Approach 2 – Linearization using SOS variables**
452 An alternative to the method using binary variables described above relies on the use of
453 Special-Ordered-Set (SOS) variables, as proposed by [37]. SOS variables are defined as
454 consecutive, ordered sets of variables. They differ from other variables in the sense that no
455 more than one (called SOS1) or two (called SOS2) adjacent elements in the ordered set can
456 take non-zero values.
457
458 By constraining their lower and upper boundaries to 0 and 1, SOS variables can be used as
459 weighting factors in linearization methods, which is the approach used in this work to
460 linearize the efficiency plane of distributed generation technologies. Unlike the binary
461 approach described in the previous section, the use of SOS variables as weighting factors
462 allows selecting either single tabled values or interpolating between two pre-defined
463 operational load levels.
464
465 Although the direct use of binary variables is avoided, using SOS requires a MILP solver
466 capable of dealing with this special type of variables. This is due to the fact that the SOS
467 restrictions, forcing a maximum of one or two non-zero adjacent values, are modeled
468 internally by the solver with auxiliary sets of binary variables [28], [38]. In this work, the
469 CPLEX solver was used, which can automatically detect SOS structures in problem
470 formulations, even if not explicitly declared, and adapt the branch-and-bound procedure
471 accordingly [39].
472

473 Eq. 13 describes how the electrical efficiency, defined as a function of P_{inst} and U_t, can be
474 approximated in each time step t using the SOS2 variables $x_{n,m,t}$:
475

476 $$\eta_{el,t} = f(P_{inst}, U_t) = \sum_n \sum_m f(P^{\wedge}_{inst,n}, U^{\wedge}_{n,m}) \cdot x_{n,m,t} = \sum_n \sum_m \eta^{\wedge}_{el,n,m} \cdot x_{n,m,t} \text{ for } t=\{1,2,...,T\}$$
477 (13)
478

479 where the weighting variables $x_{n,m,t}$ are defined as positive variables with:
480

481 $0 \leq x_{n,m,t} \leq 1$ for n={1, 2,..., N}, m={1, 2,…, M} and t={1, 2,…, T}   (14)
482

483 As previously mentioned, solving the operational efficiency for DER technologies depends on
484 the installed capacity and on the operational level in each time step. For this reason, a
485 distinction must be made between the two, as the installed capacity is selected from the N
486 discrete capacity options and the operational level can be a continuous value interpolated
487 between two consecutive M levels. Thus, a SOS1 condition is used to solve the installed
488 capacity and a SOS2 condition is used to find the operational load level, as illustrated in Fig.
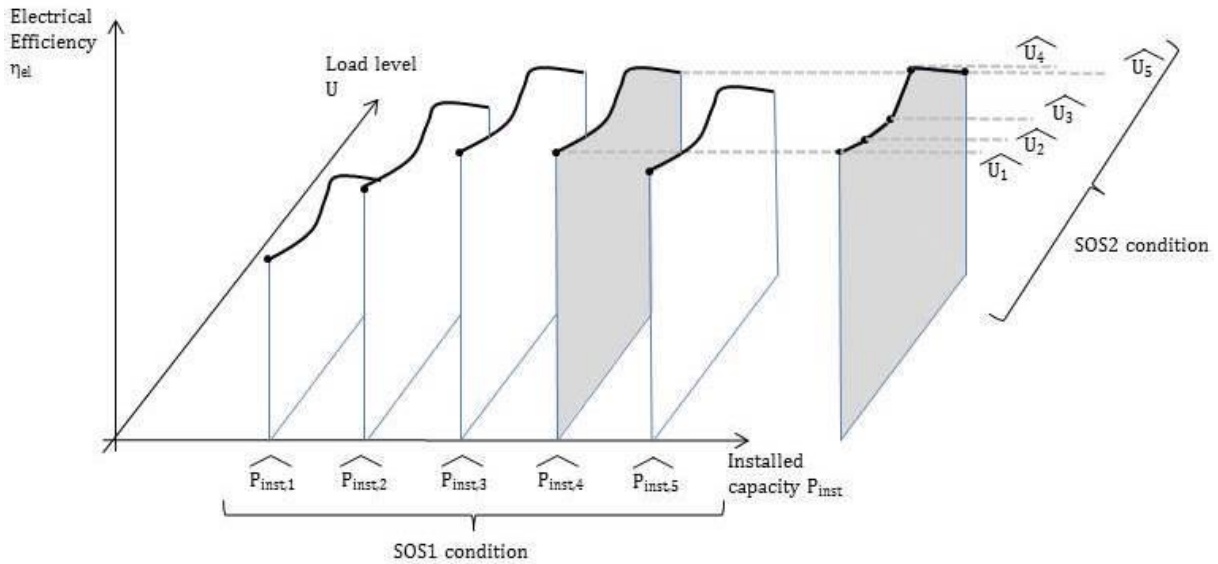489 6.
490

491
492 *Fig.6. Schematic of the approach based on SOS variable declarations to choose efficiencies*
493 *changing with installed capacity P_{inst} and operational load level U_t at each time step t*

494 In this figure, the selection of the installed capacity from the discrete set is represented by the
495 different "slices" for each tabled capacity. Once a capacity is chosen (in Fig. 6 this would be
496 the installed capacity $P^{\wedge}_{inst,4}$ highlighted in grey), the load level can be determined over time.
497 In practice, the goal is to allow load levels to be any continuous number between a minimum
498 part-load threshold and 1, representing the load operation range allowed for each technology.
499

500 In the tabled values, each U_t level stands for a discrete point within the available operational
501 load range and the use of SOS variables allows a better representation by creating the
502 possibility of interpolating between two consecutive tabled load levels. E.g., if load levels are
503 tabled with a resolution of 10%, the relevant efficiency for 75% load operation could be
504 obtained by interpolating between the values pre-defined for 70% and 80% load. This is done
505 using variables $x_{n,m,t}$ under an SOS2 constraint in the m-dimension:
506

507 $\sum_m x_{n,m,t} = 1 \text{ and } x_{n,m,t} + x_{n,m-1,t} \geq 0$ for up to two elements (SOS2)   (15)

508
509 As stated above, no more than two consecutive elements within the SOS2 are allowed to be
510 non-zero. Since the sum of all $x_{n,m,t}$ in the n- and m-dimension has to be 1, single tabled values
511 can be chosen (if $x_{n,m,t} = 1$) or interpolated between them (two consecutive $x_{n,m,t}$ values add up
512 to 1 in the m-dimension).
513
514 As stated above, the selection of a discrete capacity P_{inst} requires the use of a SOS1 condition
515 in the n-dimension. However, the GAMS platform used to implement DER-CAM does not
516 support this directly: Only the last index can be assigned to an SOS variable. Therefore, an
517 auxiliary binary variable y_n is introduced to allow only one variable to be non-zero in the n-
518 dimension of $x_{n,m,t}$ by applying Eq. 16 and 17:
519
520 $\sum_m x_{n,m,t} = y_n$ for n={1,2,…,N} and t={1,2,…,T}   (16)
521
522 $\sum_n y_n = 1$ (17)
523
524 The same method can be used to exclude load levels between the minimum threshold and
525 zero. By assigning a binary variable to this range, only zero or the minimum load can be
526 achieved. Also, since the sum of all $x_{n,m,t}$ values has to be 1, it is important to always define
527 "placeholders" with a zero load and a zero capacity, in case the unit is not installed and/or not
528 operated at a certain point in time.
529
530 Similarly to the binary variable technique, $x_{n,m,t}$ is also used as a pointing variable when using
531 SOS variables to indicate the chosen or interpolated tabled values for the electricity
532 generation, fuel consumption and heat output. Eq. 18 shows the calculation of the supplied
533 electricity at time step t as an example:
534
535 $P_{el,t} = \sum_n \sum_m P^{\wedge}_{el,n,m} \cdot x_{n,m,t}$ for t= {1,2,…,T}   (18)
536
537 It should be noted that all these equations have to be solved for each time-step t, expressed in
538 all variables. The installed capacity, which remains constant over time, is given by Eq. 19:
539
540 $P_{inst} = \sum_n \sum_m P^{\wedge}_{inst,n} \cdot x_{n,m,t}$ for t={1,2,…,T}   (19)
541
542 The main advantage of this approach is the flexibility in using the tabled values. Interpolation
543 is allowed between different load levels, and further constraints such as a minimum load can
544 be easily implemented. Thus, the results obtained using this approach should be more precise
545 than using Approach 1. Furthermore, solvers such as CPLEX apply adapted branch-and-
546 bound procedures for SOS variables, which can have positive influence on the calculation
547 time [38]. On the downside, more variables are required for this approach, such as the SOS1
548 variable y_n. This in return increases the complexity of the problem, and therefore, the overall
549 processing time may become longer even considering the improved performance in SOS-
550 enabled solvers. It further should be noted that not all MILP solvers can handle SOS
551 variables, and that their internal definition might even differ from solver to solver [40]. It is
552 therefore advised to consult the respective solver manual before applying this approach.
553 Additionally, the general drawbacks mentioned in the binary approach concerning the overall
554 flexibility of the methodology also apply: Both approaches result in considerably less flexible
555 models and require more user intervention.
556

557 The following chapters describe the integration of both approaches into DER-CAM and a
558 comparison is conducted based on several case studies.
559

5. Modelling effects of considering variable efficiencies
560

561 In order to evaluate the effects of variable efficiencies on energy system models and to be
562 able to compare these approaches, they both have been integrated into DER-CAM and applied
563 for several case studies. In the following sections the implementation of both approaches into
564 DER-CAM, relevant input data and assumptions, as well as the results of various simulations
565 are presented. The chapter concludes with a discussion of the observations.

5.1. Implementation into DER-CAM
566

567 The problem solved by DER-CAM is formulated using GAMS, which is commonly used for
568 large scale modeling applications. It allows creating high level mathematical formulations and
569 converts them to representations required by specific third-party solvers such as CPLEX,
570 MINOS, or BARON. It can be used to model and solve various mathematical programs
571 including linear (LP), non-linear (NLP), mixed integer linear (MILP) and mixed integer non-
572 linear programs (MINLP) [41]. Both the binary and SOS variables approaches described in
573 this paper are directly supported by GAMS, although SOS variables are a special feature and
574 not all MIP solvers available through GAMS support them.
575

576 Both the binary and SOS variable approaches were implemented in the latest Investment &
577 Planning (I&P) version of DER-CAM (v4.1.1), which considers advanced features including
578 investments in passive building components, such as windows and insulation.
579 As stated in Chapter 2, I&P DER-CAM finds optimal solutions for microgrid and building
580 energy supply systems, considering investments in energy supply and storage technologies,
581 and this is done by sampling three typical days for each month or a typical year, resulting in a
582 total of 36 days of hourly loads. Along with investment decisions, all energy outputs, fuel
583 consumption, CO_2 emissions, and other operating schedules are determined by DER-CAM
584 and reported for this reference year.
585

586 Due to the current structure of DER-CAM, both approaches presented to model non-linear
587 efficiency curves have to be adapted to ensure their implementation and several pre-
588 calculations have to be made. Fig. 7 shows an overview of how both approaches are
589 integrated and the corresponding data handling. Specifically, the user specifies efficiencies for
590 certain partial loads and installed capacity sizes for each technology and relevant fuel type
591 (light shaded on the left upper corner of the graphic). This data is highly relevant since the
592 efficiency characteristics can differ significantly depending on the fuel used, even for the
593 same technology. In this work, three efficiency tables were specified for the ICE, MT and FC,
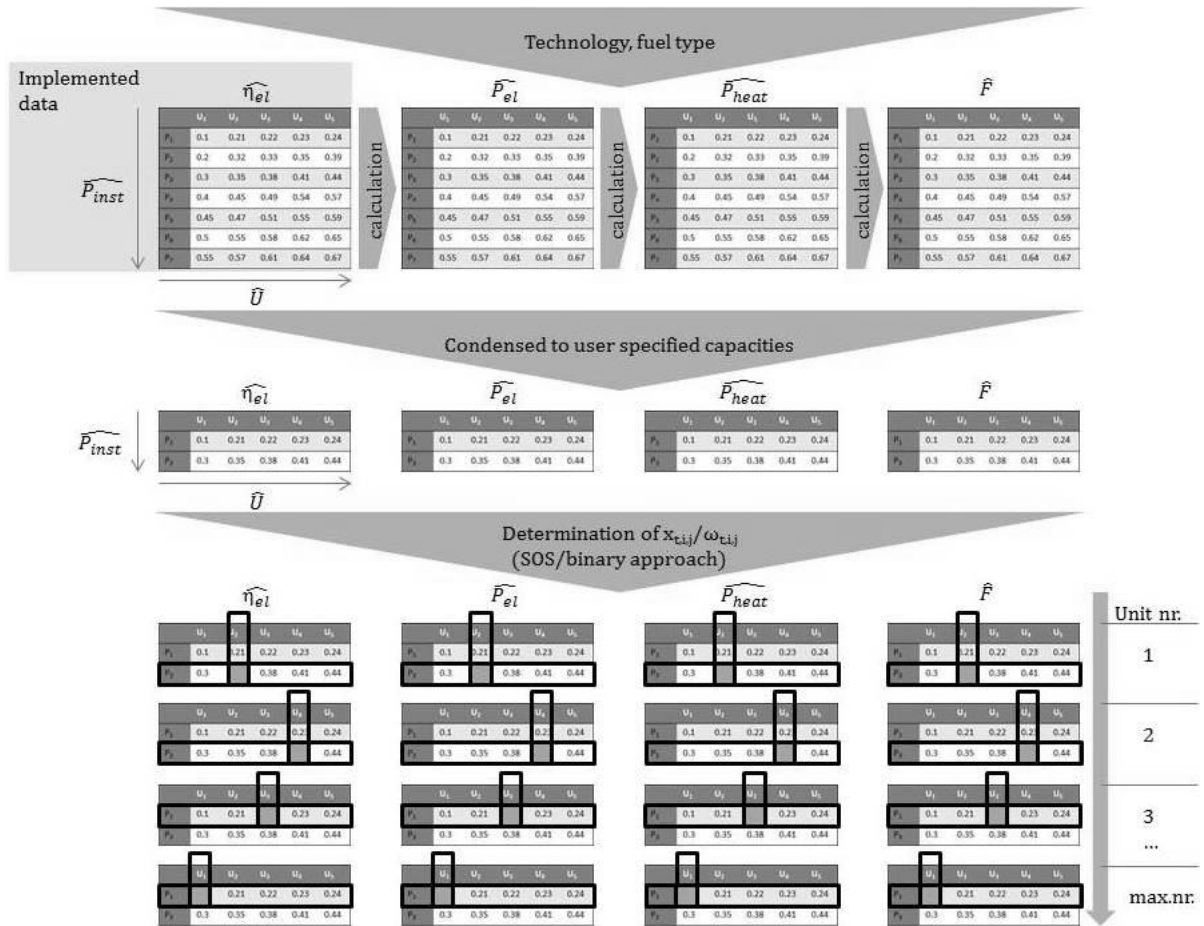594 all three assuming natural gas operation.
595

596
597 *Fig. 7. Schematic of the implementation of the approach using SOS and binary variables in*
598 *DER-CAM*

599 Given the specified efficiency table for each size and load level, DER-CAM calculates the
600 corresponding values for electricity output, fuel consumption and, if relevant, heat output. As
601 part of the DER-CAM structure, users specify desired sizes of each technology in another part
602 of the model. Consequently, the efficiency table is in a first step condensed to these sizes to
603 avoid unnecessary calculations. When all data is pre-processed the actual optimization
604 process is launched. The binary or SOS weighting variables are determined for each
605 technology and calculation step t, determining the load levels for all points in time. As
606 mentioned earlier, the variables are used to obtain values for all four data tables, marked in
607 the figure with black boxes for the chosen index of P_{inst} and U_t. The light shaded box indicates
608 the resulting value in the table.

609

610 In addition to the above description, the structure of DER-CAM considers another dimension:
611 the number of units, k, since the model allows for more than one unit of each size and
612 technology to be installed, and determines the optimal number k for each technology as part
613 of the solution. This additional dimension requires that a maximum number of components
614 are implemented in the model, and in this work 15 units have been set as a limit for each
615 technology. DER-CAM applies the presented approaches for each unit up to the maximum
616 number, determining if the unit should be installed and operated at a certain time t or not. This
617 is indicated in Fig. 7 on the lower right part. As an example, the equation for the electricity
618 output of the approach using SOS2 variables is adapted in Eq. 20 by adding another index k to
619 the weighting variable referring to the number of installed units.

620

621 $P_{el,t,k} = \sum_n \sum_m P^\wedge_{el,n,m} \cdot x_{n,m,t,k}$ for t={1,2,…T} and k={1,2,…,K} (20)
622
623 The other equations for both approaches are adapted accordingly, adding the indices *t* and *k*.
624

5.2. Input data and assumptions

626 As stated above, DER-CAM decides on the optimal energy supply system configuration using
627 several input data for one reference year. The main inputs are [42]:
628

629 • hourly building loads for electricity, heating, cooling, domestic hot water and cooking
630 • natural gas and electricity prices
631 • local solar radiation
632 • CO_2 emission factors for utilities to evaluate CO_2 mitigation by local energy supply
633 • performance and cost data of building equipment including energy supply
634   technologies
635

636 Additionally, as mentioned in chapter 4, the approaches now introduced require user
637 specifications on the efficiency curves of each technology and applied fuel. Other parameters,
638 such as electricity generation and fuel consumption, are calculated based on these efficiencies.
639 The heat output is determined based on the assumption that the overall efficiency of all three
640 technologies considered in this paper is constant for all load levels. This simplification is
641 reasonable, as lower part load efficiency levels lead to more waste heat. When this happens
642 the heat to power ratio increases (greater amount of heat recovered and lower power output),
643 which is compatible with a constant overall efficiency, as illustrated in Eq. 21. This equation
644 shows how the heat output table is determined for both approaches based on Eq. 4 and 5 and a
645 constant overall efficiency for each capacity:
646

647 $P^\wedge_{heat,n,m} = \frac{\eta_{overall,n} - \eta^\wedge_{el,n,m}}{\eta^\wedge_{el,n,m}} \cdot P^\wedge_{el,n,m}$ for n={1, 2,…, N}, m={1, 2,…, M}, t={1,2,…T},
648 k={1,2,…,K} (21)
649

650 This method for calculating CHP efficiency, known simply as *total system efficiency*, is the
651 most commonly used approach and an adequate method to compare CHP efficiency to the
652 efficiency of a system with separate heat and power production. In situations where the
653 electrical efficiency of CHP is being compared with conventional power production, the
654 alternative *effective electric efficiency* metric should be used. As DER-CAM considers
655 simultaneously different end-use loads including both power and heating, and different
656 options to meet these loads are present in the model, the total system efficiency method is
657 better suited.
658

659 The improvements made to DER-CAM to model non-linear efficiency curves were analysed
660 by performing a case study with a number of selected buildings, which have been previously
661 analysed using DER-CAM in the report "Encouraging Combined Heat and Power in
662 California Buildings" [42]. The results from this report were used as a reference for
663 comparison when evaluating the effects of considering variable efficiencies.
664

665 According to [42], building load profiles were obtained from the California Commercial End-
666 Use Survey [43] for four building types in the city of San Francisco. The facilities
667 investigated are a large lodging (LLODG), a large office building (LLOFF), a medium-sized
668 office building (MLOFF) and a large warehouse (LWRHS). In the reference report several

669   run sets with different objectives and frame conditions have been performed [42]. In this
670   paper, test runs "4e10" from the report have been chosen, where the objective function was to
671   minimize overall building CO_2 emissions considering a maximum global payback time of 10
672   years for DER investments. Thus, equation 2 as described earlier in this paper is applied as
673   the objective function.
674
675   Key results obtained in this run suggested the installation of Fuel Cell Systems with a Heat
676   Exchanger (FC-HX) and Micro-turbines with a Heat Exchanger (MT-HX) as the CO_2 optimal
677   solution. Their technical specifications together with the relevant cost data are listed in Table
678   3 and are taken from [42].
679
680   Table 3. Technical specifications of investigated CHP technologies [42]
681

Technology	Electrical capacity [kW]	Lifetime [Years]	Capital cost [$/kW]	Maintenance cost [$/kWh]	Full load electric efficiency [%]	Heat-to-Power ratio α [-]
MT-HX	60	10	1,584	0.017	31	1.8
MT-HX	150	10	1,290	0.017	33	1.4
FC-HX	100	10	4,192	0.033	60	0.53
FC-HX	250	10	3,359	0.033	60	0.53

682   *MT: micro-turbine, FC: fuel cell, HX: heat exchanger for waste heat utilization*
683
684   Part load efficiency data for natural gas powered MT and FC was taken from reports [44] and
685   [45]. All data was slightly scaled to match the full load electrical efficiencies already specified
686   in DER-CAM as indicated in Table 3. Table 4 defines the part load performance for two
687   capacities of a natural gas powered micro-turbine, which are considered in the model.
688   Analysing the data in this table shows that the maximum efficiency for the large 150 kW
689   micro-turbine at full load is slightly higher than for the smaller 60 kW unit. The implemented
690   minimum load for the fuel cell is 30% and for the micro-turbine 10%.
691
692   Table 4. Electrical efficiencies of natural gas powered MT [44]
693

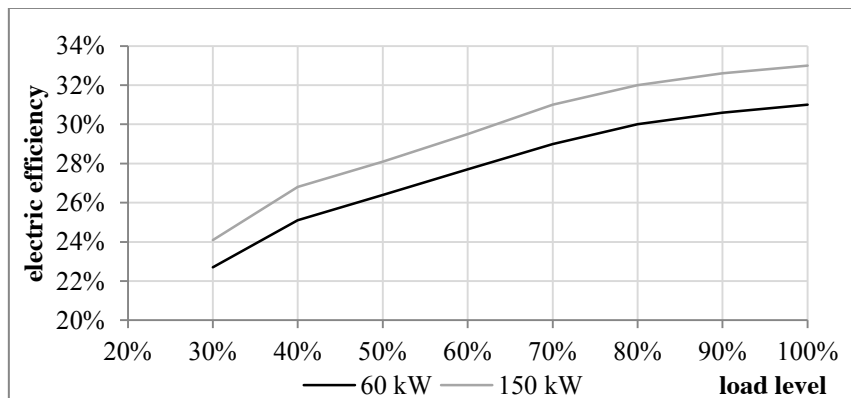| Installed capacity		Load level								
		$U_{1,t}$ 0%	$U_{2,t}$ 30%	$U_{3,t}$ 40%	$U_{4,t}$ 50%	$U_{5,t}$ 60%	$U_{6,t}$ 70%	$U_{7,t}$ 80%	$U_{8,t}$ 90%	$U_{9,t}$ 100%
P_1	60 kW	0	0.227	0.251	0.264	0.277	0.29	0.3	0.306	0.31
P_2	150 kW	0	0.241	0.268	0.281	0.295	0.31	0.32	0.326	0.33

694

695

696   *Fig. 8. Electrical efficiencies for natural gas powered Micro Turbines*

697
698   Table 5 indicates the part load efficiencies for both Fuel Cell capacities considered in this
699   work. According to [42], maximal efficiency for both unit sizes is considered equal. The
700   tabled values reveal that the slope of the performance curve is close or even equal to zero in
701   the range of load levels between 60% and 100%.

702
703   Table 5. Electrical efficiencies of natural gas powered Phosphoric Acid FC [45]
704

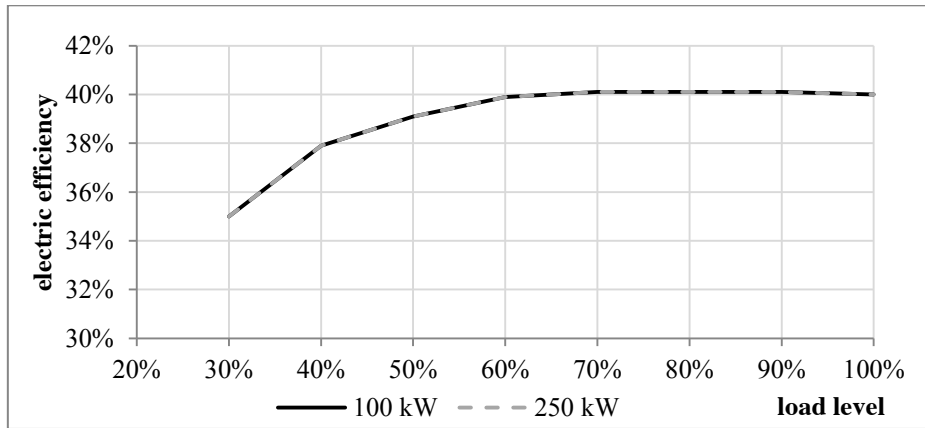| Installed capacity	Load level								
	$U_{1,t}$ 0%	$U_{2,t}$ 30%	$U_{3,t}$ 40%	$U_{4,t}$ 50%	$U_{5,t}$ 60%	$U_{6,t}$ 70%	$U_{7,t}$ 80%	$U_{8,t}$ 90%	$U_{9,t}$ 100%
P_1 100 kW	0	0.35	0.379	0.391	0.399	0.401	0.401	0.401	0.4
P_2 250 kW	0	0.35	0.379	0.391	0.399	0.401	0.401	0.401	0.4

705

706
707   *Fig. 9. Electrical efficiencies for natural gas powered Phosphoric Acid FC*
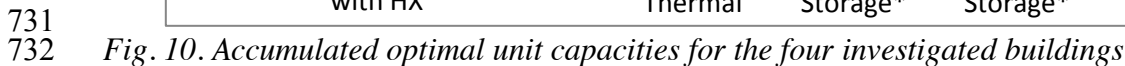
708
709   In the standard version of DER-CAM, minimum load levels were implemented to limit the
710   impacts of the simplification involving constant efficiencies. This resulted in a rather
711   conservative minimum load level of 90% for the fuel cell, which was lowered to a minimum
712   operational load level of 30% in this work, as a result of considering variable efficiencies.

713
714   Based on the input data presented, four different optimization runs were performed for each of
715   the two methods described to incorporate non-linear efficiency curves. Additionally, the four
716   reference cases with fixed efficiencies have been reproduced with the latest v4.1.1 DER-CAM
717   code for the purpose of model validation and solver performance comparison between all
718   approaches. Thus, a total number of 12 optimization runs have been carried out.

719
720   In the following subchapter the obtained results are presented and discussed in detail.

721

722   **5.3. Optimization results**
723   Four buildings in the city of San Francisco have been investigated, as indicated earlier. Fig.
724   10 depicts the aggregated capacities suggested by DER-CAM when considering the CO_2
725   minimization objective function in all four cases. The results are shown separately for each of
726   the approaches implemented and the results obtained with fixed efficiencies are referred to as
727   "original", representing the base case. The results obtained using binary and SOS2 variables

728 to approximate non-linear efficiencies are named correspondingly. Please note that the sizes
729 for all technologies refer to electrical capacities, except for the heat storage.
730

731

732 *Fig. 10. Accumulated optimal unit capacities for the four investigated buildings*

733 Results shown in Fig. 10 indicate that the CHP (MT and FC with HX) capacities obtained
734 using the binary approach and the benchmark constant efficiency methods differ only slightly.
735 A larger deviation can be observed when using SOS2 variables to model variable efficiencies.
736 Despite these differences, the ratio between installed fuel cells and micro-turbines is almost
737 constant for both proposed methods. In all buildings and methods used, discrete-sized
738 generation technologies selected by DER-CAM were equipped with heat exchangers to allow
739 CHP operation. Besides MT and FC, PV modules and solar thermal collectors were also part
740 of the solutions found in all cases.
741
742 It can also be observed that the capacity of DER technologies found by DER-CAM is only
743 slightly affected by the consideration of variable efficiencies. Fluctuations between the
744 approaches for PV and ST installations are only minor. Changes for the battery storage
745 capacities are negligible. The largest observed impact occurred on heat storage, where the use
746 of the binary approach led to optimal installed capacities nearly twice the size of those
747 obtained in the base case.
748
749 The reasons for the observed differences can be explained when investigating the results in
750 greater detail. Tables 6 and 7 lists detailed results for all cases.
751
752 Table 6. Detailed simulation results for the first two buildings and all three approaches

Building case	*LLODG*			*LLOFF*		
Approach	Original	Binary	SOS2	Original	Binary	SOS2
CO$_2$ emissions						

Total Annual CO_2 emissions [kg]	1.805.483	1.758.140	2.122.843	3.548.091	3.560.468	3.529.838
Costs						
Total Annual Energy Costs [$]	697,702	707,919	761,750	1,113,650	1,117,604	1,117,581
Installed Capacities						
FC-HX [kW]	600	500	0	0	0	0
MT-HX [kW]	60	60	180	330	390	300
CHP total [kW]	660	560	180	330	390	300
PV [kW]	205	222	227	686	661	651
Solar Thermal [kW]	1,238	1,355	1,331	0	0	0
Battery Storage [kWh]	0	233	0	0	0	0
Heat Storage [kWh]	1,776	2,527	1,920	0	490	463
Energy Generation						
CHP Electricity Generation [kWh]	4,998,619	4,314,180	1,021,172	1,901,746	2,217,300	1,901,035
CHP Heat Generation [kWh]	2,630,717	2,418,665	1,838,646	2,999,596	3,429,561	3,296,313
CHP fuel consumption [kWh]	8,428,554	7,326,588	3,294,721	6,020,685	7,045,543	6,141,124
Model Performance and Key Data						
CPU time [s]	129	23,383	189,321	158	23,368	145,287
Variables [-]	523,307	1,791,659	2,102,699	523,307	1,791,659	2,102,699
Equations [-]	293,353	441,961	753,001	293,353	441,961	753,001

753

754   Table 7. Detailed simulation results for the last two buildings and all three approaches

Building case	*MLOFF*			*LWRHS*		
Approach	Original	Binary	SOS2	Original	Binary	SOS2
CO$_2$ emissions						
Total Annual CO$_2$ emissions [kg]	891.974	196.201	877.663	Missing	Missing	171.302
Costs						
Total Annual Energy Costs [$]	484,024	503,673	484,138	131,046	122,984	121,266
Installed Capacities						
FC-HX	250	0	350	100	100	100
MT-HX	60	210	0	0	0	0
CHP total [kW]	310	210	350	100	100	100
PV [kW]	823	872	731	173	198	201
Solar Thermal [kW]	133	206	131	3	1	0
Battery Storage [kWh]	502	471	686	571	372	319
Heat Storage [kWh]	0	534	0	0	0	0
Energy Generation						
CHP Electricity Generation [kWh]	1,873,291	763,392	2,520,372	574,120	520,960	523,450
CHP Heat Generation [kWh]	1,103,721	1,130,125	1,338,894	51,738	51,794	51,940
CHP fuel consumption [kWh]	3,394,010	2,372,110	4,211,090	956,867	867,984	873,318
Model Performance and Key Data						
CPU time [s]	2,426	23,536	163,740	21,393	84,334	77,479
Variables [-]	523,307	1,791,659	2,102,699	523,307	1,791,659	2,102,699
Equations [-]	293,353	441,961	753,001	293,353	441,961	753,001

755
756   When investigating the total annual energy costs listed on the top of Tables 6 and 7, it is
757   observed that these are barely affected by considering flexible efficiencies. The used solver
758   precision was five percent for which reason deviations in the optimal result lower or equal
759   than this value are in the precision range and do not necessarily reflect changes induced by the
760   approaches applying variable efficiencies. The largest deviation can be found for the LLODG
761   building when using the SOS2 based approach. Otherwise, the changes of total costs are close
762   to zero. Likewise, as already concluded from the figure above, the average of installed
763   capacities does not deviate largely from the reference scenario. Solely the size of the CHP
764   units for the LLODG building is dramatically lower for the approach using SOS2 variables.

765
766   Concerning storage technologies, a large increase can be observed for the hot water tank, as
767   stated earlier. This is mainly due to a greater ability to generate heat, as the heat-to-power
768   ratio increases during part load operation. This is a direct consequence of considering variable
769   efficiencies, as lower electric efficiencies result in a higher ability to recover heat when
770   compared to the original case where the heat-to-power ratio is assumed to be constant.
771   Another reason for the increased importance of heat storage is the change in technology
772   investment. Tables 6 and 7 indicate that MTs are more favorable in the adapted approaches
773   while FC capacities decrease. Thus, due to the very different heat-to-power ratios of the MT
774   and FC, the overall ratio between heat and electricity changes significantly from one case to

775 the other. Namely, the applied micro-turbine has a much larger heat-to-power ratio than the
776 considered FC system. These characteristics are also the reason for a strong decline in the
777 electricity generation for the MLOFF building with the applied binary approach, despite a
778 slight increase in heat supply. Despite the minor changes in total heat supply, the large
779 increase in heat storage might be a consequence of the considerable larger amounts of
780 supplied heat per hour, including solar thermal and the micro-turbine. Thus, it can be
781 concluded that two factors have an impact on the heat supply rates and consequently heat
782 storage size:

784 1) Changes in the part load heat-to-power ratio and
785 2) Changes in the overall heat-to-power ratio of the system due to different technology
786 capacities.

788 As stated earlier, overall investment costs are hardly affected by including variable
789 efficiencies in the optimization process. However, operational performance of all relevant
790 technologies is different, which would suggest different system costs. Thus, the results
791 indicate that changes in the technology mix, in this case towards larger microturbine
792 installations, compensate for variations observed in operational performance. .

794 In the last part of both above tables key data for the optimization models is listed. The
795 required CPU time increased for all the cases considerably. The largest changes can be
796 observed for the approach using SOS2 variables, which had longer running times up to the
797 factor 10^6. The binary approach solved generally faster than the SOS2 alternative. However, it
798 was still considerably slower than the reference cases with run time increases in the range of
799 10^2 to 10^4. As a conclusion, it can be stated that both approaches cause considerably longer
800 calculation times with the SOS2 approach having the largest increase.

802 **5.4. Modelling with variable vs. non-variable efficiencies**
803 As discussed in the previous section, both modelling approaches only have limited impacts on
804 the objective function. However, calculation time and complexity of the model increase
805 considerably. Therefore, it is crucial for researchers and system designers to evaluate the
806 impacts and consequently the need for the presented approaches before applying them in a
807 specific building optimization. The efficiency data tables presented earlier (Table 2, 4 and 5)
808 indicated that deviations from the original approach only occur in part loads, for which full
809 load efficiency cannot be achieved. Fig. 11 depicts the share of the total accumulated amount
810 of hours of operation of installed units for all four investigated buildings distinguished by the
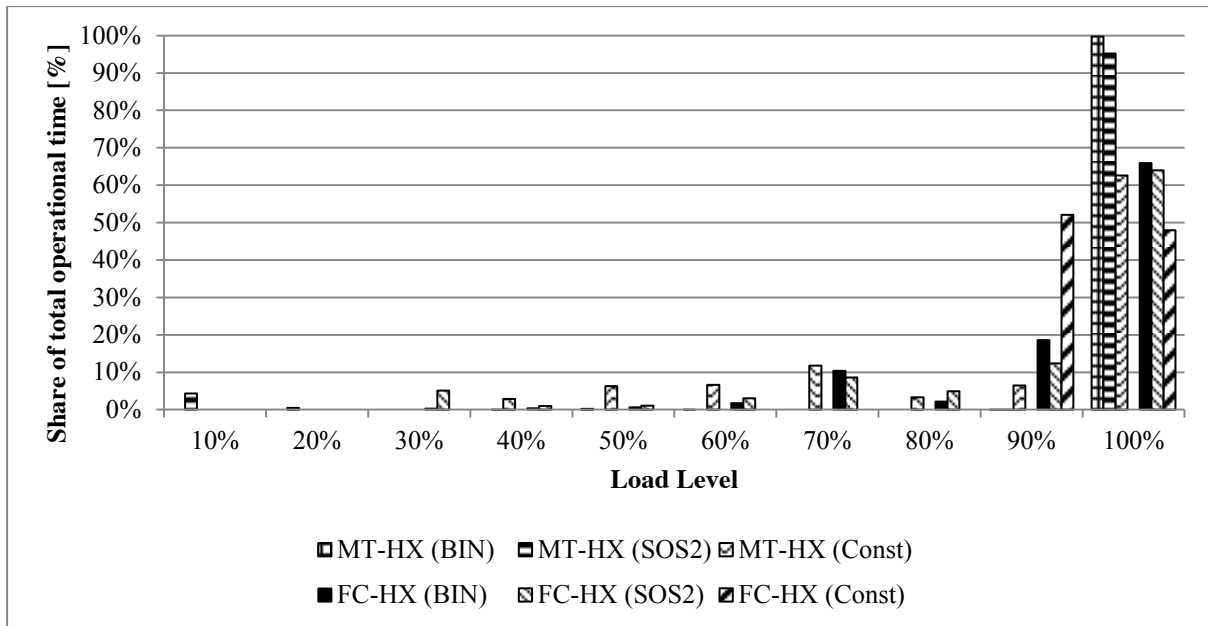811 corresponding load levels.

Fig. 11. Accumulated hours of operation for all buildings at relevant load levels compared by applied modelling approach

This figure indicates that the units were mostly used in full load operation for both approaches. Further, distinction between the fuel cell and the micro-turbine modelling is visible. The micro-turbine is almost exclusively used at full capacity. Fuel cell part load operation, however, seems to be more relevant. At load levels 30%, 70% and 90% the fuel cell is operated a considerable amount of time. Altogether, the FC units are modelled 48% and 44% of the operational time in part load using the binary and the SOS2 approach, respectively. This observation is important considering the fact that part load operation of fuel cells is limited to a minimal 90% in the original DER-CAM version considering constant efficiencies and for that reason fuel cell technology that cannot follow the load. It is also relevant to note that in DER-CAM the smallest available size for the MT is 60 kW, which is lower than the minimum installed capacity of 100 kW for the fuel cell. Further, the largest available size is 250 kW for the fuel cell and only 150 kW for the micro-turbine. This is also influencing the load performance of the components, since smaller units are more likely to run in full load. Furthermore, it should be noted that in the original DER-CAM version the micro-turbine was often used in part load operation. Taking into account the fact that originally fuel cells are limited to a minimal 90% part load it is interesting to observe that the micro-turbine is used to a similar extent of what the fuel cells are used once the binary or SOS2 methods are implemented. However, a general statement cannot be made in this work, both because of the original imposed constrains in terms of minimal load and because consumption profiles also change for each building and the determined capacities consist for several cases of combinations of small and large units. Therefore, it is recommended to investigate in future studies, if the observation made in this work can be generalized or is only valid for these specific component sizes.

Given the results of this study, it can be stated that the effect of variable efficiencies seems to be technology dependent for the given configurations. Since the micro-turbine is modelled mainly in full load, the assumption of constant efficiencies is reasonable in DER-CAM. For fuel cell technologies, however, an approach with variable efficiencies might be relevant for certain cases and technologies (e.g. PEM fuel cells) given the fact that part load modelling accounts for up to 48% of the operational time.

846 Concerning the performance of the adapted DER-CAM versions, the SOS2 approach caused
847 the largest increase in calculation time. The advantage of using SOS2 variables is that they
848 allow for interpolation between tabled load levels in the approach presented and thus might
849 lead to more precise results. Table 8 indicates the number of interpolations actually applied in
850 the optimal solutions for all four buildings dependent on the technology.
851
852 Table 8. Total number of interpolations applied in the SOS2 approach for all buildings
853

	MT-HX	FC-HX
Number of interpolations	100	279

854
855 As expected, most of the interpolations have been made for fuel cell units, resulting from part
856 load operation occurring in a significant amount of time. The micro-turbine operation
857 required interpolation in a lower number of 100 hours, which represents a very low share of
858 only 1.4%. Thus, given the large increase in computational time, the SOS2 approach does not
859 seem favorable for the building range investigated in this work. Further, it should be
860 mentioned that this approach results in a less flexible model, since SOS2 variables are not
861 supported by all solvers and their definition is different between solvers. However, for small
862 scale grid-isolated energy systems, the SOS2 approach could still be favorable, due to an
863 increased importance of part load performance. The use of the binary approach might not be
864 applicable for such specific cases, as it does not allow for interpolation, which could be
865 required to meet the building energy demand supplied by only one or two components. Thus,
866 it could lead to an infeasible problem.
867

868 **6. Conclusion and recommendations**

869 In this paper two approaches were presented to account for variable efficiencies when
870 modelling CHP technologies in distributed energy systems. Furthermore, the optimization
871 model DER-CAM was adapted to implement these features and case study optimizations have
872 been successfully performed to compare both approaches and to evaluate the effect of taking
873 variable efficiencies into account. The main findings are:
874

875 • The total annual energy costs are not subject to large changes, when considering
876   variable efficiencies.
877 • However, changes in the choice of technologies were observed. FC units were
878   replaced by MT and slightly also vice-versa. The overall installed capacities per
879   building varied moderately with one extreme example.
880 • System performance was affected considerably. Storage technologies gained increased
881   importance, with particular focus on heat storage.
882 • Further, it was found that in DER-CAM the importance of modelling variable
883   efficiencies depends on the technology. The micro-turbine was modelled 97% of the
884   time in full load, which corresponds to the original DER-CAM version with constant
885   efficiencies. On the contrary, fuel cell units were referred to being operated half of the
886   time in part load.
887 • Both approaches increased the calculation time considerably. The binary approach led
888   to processing times being 2 to 100 times longer.
889 • The SOS2 approach caused the largest increases by factors up to 10^6. Interpolations in
890   load levels were hardly applied.
891

892   •   The results show that constant efficiencies can be reasonable to model CHP
893   performance. Investment decisions were only slightly different when considering
894   variable efficiencies. However, when identifying optimal operational strategies, the
895   presented approaches can lead to recommendations that are more realistic.
896

897 Based on these conclusions, the following recommendations can be made:
898

899   •   The implementation of variable efficiencies should not be generally applied due to the
900   significant increase in computational time. An individual assessment beforehand in
901   regard to the investigation purpose should be made.
902   •   Results indicate that micro-turbines could be modelled with fixed efficiencies,
903   although further research is suggested to assess if this observation can be generalized
904   or if it is only valid for the given component sizes.
905   •   Applying variable efficiencies for fuel cells should be considered and could be subject
906   to further investigation with an increased number of buildings and locations.
907   •   When modelling variable efficiencies, the binary approach should be used with
908   processing times being considerably faster than for the SOS2 approach.
909   •   The SOS2 approach could be used for very specific cases investigating small grid-
910   isolated systems, which require a large flexibility in part load operation.
911   •   It is recommended to implement the binary approach also in the Operational version
912   of DER-CAM, since unit performance is affected and storage solutions gain
913   importance.
914

References

[1] M. Bianchi, A. De Pascale, F. Melino, and A. Peretto, "Performance prediction of micro-CHP systems using simple virtual operating cycles," *Applied Thermal Engineering*, vol. 71, no. 2, pp. 771–779, Oct. 2014.

[2] M. Bianchi and A. De Pascale, "Emission Calculation Methodologies for CHP Plants," *Energy Procedia*, vol. 14, no. 0, pp. 1323–1330, 2012.

[3] B. Thomas, "Benchmark testing of Micro-CHP units," *Applied Thermal Engineering*, vol. 28, no. 16, pp. 2049–2054, Nov. 2008.

[4] M. Ebrahimi, A. Keshavarz, and A. Jamali, "Energy and exergy analyses of a micro-steam CCHP cycle for a residential building," *Energy and Buildings*, vol. 45, pp. 202–210, Feb. 2012.

[5] X. Q. Kong, R. Z. Wang, Y. Li, and X. H. Huang, "Optimal operation of a micro-combined cooling, heating and power system driven by a gas engine," *Energy Conversion and Management*, vol. 50, no. 3, pp. 530–538, Mar. 2009.

[6] D. W. Wu and R. Z. Wang, "Combined cooling, heating and power: A review," *Progress in Energy and Combustion Science*, vol. 32, no. 5–6, pp. 459–495, Sep. 2006.

[7] G. Kayo, A. Hasan, and K. Siren, "Energy sharing and matching in different combinations of buildings, CHP capacities and operation strategy," *Energy and Buildings*, vol. 82, pp. 685–695, Oct. 2014.

[8] C. Milan, C. Bojesen, and M. P. Nielsen, "A cost optimization model for 100% renewable residential energy supply systems," *Energy*, vol. 48, no. 1, pp. 118–127, Dec. 2012.

[9] M. Münster, P. E. Morthorst, H. V. Larsen, L. Bregnbæk, J. Werling, H. H. Lindboe, and H. Ravn, "The role of district heating in the future Danish energy system," *Energy*, vol. 48, no. 1, pp. 47–55, Dec. 2012.

[10] H. Lund, B. Möller, B. V. Mathiesen, and A. Dyrelund, "The role of district heating in future renewable energy systems," *Energy*, vol. 35, no. 3, pp. 1381–1390, Mar. 2010.

[11] P. Liu, E. N. Pistikopoulos, and Z. Li, "An energy systems engineering approach to the optimal design of energy systems in commercial buildings," *Energy Policy*, vol. 38, no. 8, pp. 4224–4231, Aug. 2010.

[12] H. Ren and W. Gao, "A MILP model for integrated plan and evaluation of distributed energy systems," *Applied Energy*, vol. 87, no. 3, pp. 1001–1014, Mar. 2010.

[13] A. D. Hawkes and M. A. Leach, "Modelling high level system design and unit commitment for a microgrid," *Applied Energy*, vol. 86, no. 7–8, pp. 1253–1265, Jul. 2009.

[14] E. Thorin, H. Brand, and C. Weber, "Long-term optimization of cogeneration systems in a competitive market environment," *Applied Energy*, vol. 81, no. 2, pp. 152–169, Jun. 2005.

[15] H. Cho, S. D. Eksioglu, R. Luck, and L. M. Chamra, "Operation of a cchp system using an optimal energy dispatch algorithm," in *ASME 2008 2nd International Conference on Energy Sustainability collocated with the Heat Transfer, Fluids Engineering, and 3rd Energy Nanotechnology Conferences*, 2008, pp. 747–754.

[16] H. Cho, P. J. Mago, R. Luck, and L. M. Chamra, "Evaluation of CCHP systems performance based on operational cost, primary energy consumption, and carbon dioxide emission by utilizing an optimal operation scheme," *Applied Energy*, vol. 86, no. 12, pp. 2540–2549, Dec. 2009.

[17] L. Wang and C. Singh, "Stochastic combined heat and power dispatch based on multi-objective particle swarm optimization," *International Journal of Electrical Power & Energy Systems*, vol. 30, no. 3, pp. 226–234, 2008.

[18] B. Mohammadi-Ivatloo, M. Moradi-Dalvand, and A. Rabiee, "Combined heat and power economic dispatch problem solution using particle swarm optimization with time varying acceleration coefficients," *Electric Power Systems Research*, vol. 95, pp. 9–18, Feb. 2013.

[19] P. K. Roy, C. Paul, and S. Sultana, "Oppositional teaching learning based optimization approach for combined heat and power dispatch," *International Journal of Electrical Power & Energy Systems*, vol. 57, pp. 392–403, May 2014.

[20] S. S. Sadat Hosseini, A. Jafarnejad, A. H. Behrooz, and A. H. Gandomi, "Combined heat and power economic dispatch by mesh adaptive direct search algorithm," *Expert Systems with Applications*, vol. 38, no. 6, pp. 6556–6564, Jun. 2011.

[21] R. Azizipanah-Abarghooee, T. Niknam, M. A. Bina, and M. Zare, "Coordination of combined heat and power-thermal-wind-photovoltaic units in economic load dispatch using chance-constrained and jointly distributed random variables methods," *Energy*, Nov. 2014.

[22] T. Guo, M. I. Henwood, and M. van Ooijen, "An algorithm for combined heat and power economic dispatch," *Power Systems, IEEE Transactions on*, vol. 11, no. 4, pp. 1778–1784, 1996.

[23] F. J. Rooijers and R. A. van Amerongen, "Static economic dispatch for co-generation systems," *Power Systems, IEEE Transactions on*, vol. 9, no. 3, pp. 1392–1398, 1994.

[24] G. Cardoso, M. Stadler, M. C. Bozchalui, R. Sharma, C. Marnay, A. Barbosa-Póvoa, and P. Ferrão, "Optimal investment and scheduling of distributed energy resources with uncertainty in electric vehicle driving schedules," *Energy*, vol. 64, no. 0, pp. 17–30, Jan. 2014.

[25] M. Stadler, M. Groissböck, G. Cardoso, and C. Marnay, "Optimizing Distributed Energy Resources and building retrofits with the strategic DER-CAModel," *Applied Energy*, vol. 132, pp. 557–567, Nov. 2014.

[26] M. Stadler, M. Kloess, M. Groissböck, G. Cardoso, R. Sharma, M. C. Bozchalui, and C. Marnay, "Electric storage in California's commercial buildings," *Applied Energy*, vol. 104, pp. 711–722, Apr. 2013.

[27] G. Cardoso, M. Stadler, A. Siddiqui, C. Marnay, N. DeForest, A. Barbosa-Póvoa, and P. Ferrão, "Microgrid reliability modeling and battery scheduling using stochastic linear programming," *Electric Power Systems Research*, vol. 103, pp. 61–69, Oct. 2013.

[28] "DER-CAM official website," 29-Jan-2014. [Online]. Available: <https://building-microgrid.lbl.gov/projects/der-cam. [Accessed: 29-Jan-2014].

[29] M. Stadler, A. Siddiqui, C. Marnay, H. Aki, and J. Lai, "Control of greenhouse gas emissions by optimal DER technology investment and energy management in zero-net-energy buildings," *European Transactions on Electrical Power*, vol. 21, no. 2, pp. 1291–1309, 2011.

[30] M. Stadler, C. Marnay, G. Cardoso, T. Lipman, O. Mégel, S. Ganguly, A. Siddiqui, and J. Lai, "The CO2 abatement potential of California's mid-sized commercial buildings," Ernest Orlando Lawrence Berkeley National Laboratory, Berkeley, CA (US), 2009.

[31] F. J. Rubio, A. S. Siddiqui, C. Marnay, and K. S. Hamachi, "CERTS customer adoption model," 2000.

[32] M. Stadler, "Effect of Heat and Electricity Storage and Reliability on Microgrid Viability: A Study of Commercial Buildings in California and New York States," 2009.

[33] C. Marnay, G. Venkataramanan, M. Stadler, A. Siddiqui, R. Firestone, and B. Chandran, "Optimal technology selection and operation of microgrids in commercial buildings," 2007, pp. 1–7.

1019 [34] G. Cardoso, M. Stadler, M. Chehreghani Bozchalui, R. Sharma, C. Marnay, A. Barbosa-
1020   Povoa, and P. Ferrao, "Stochastic programming of vehicle to building interactions with
1021   uncertainty in PEVs driving for a medium office building," 2013, pp. 7648–7653.
1022 [35] "BHKW-Kenndaten 2011," ASUE Arbeitsgemeinschaft für sparsamen und
1023   umweltfreundlichen Energieverbrauch e.V., 2011.
1024 [36] "Technology Characterization: Reciprocating Engines," Environmental Protection
1025   Ageny - Combined Heat and Power Partnership Program, Dec. 2008.
1026 [37] E. M. L. Beale and J. A. Tomlin, "Special facilities in a general mathematical
1027   programming system for non-convex problems using ordered sets of variables," *OR*, vol.
1028   69, pp. 447–454, 1970.
1029 [38] "AIMMS Modeling Guide - Integer Programming Tricks." Paragon Decision
1030   Technology B.V, 2012.
1031 [39] "IBM developerWorks - official forum," 10-Jan-2014. [Online]. Available:
1032   https://www.ibm.com/developerworks/community/forums/html/public?lang=en.
1033   [Accessed: 10-Jan-2014].
1034 [40] B. A. McCarl, A. Meeraus, P. van der Eijk, M. Bussieck, S. Dirkse, P. Steacy, and F.
1035   Nelissen, "McCarl GAMS user guide," *GAMS Development Corporation*, 2013.
1036 [41] GAMS Development Corporation, "GAMS_ A User's Guide." GAMS Development
1037   Corporation, 2010.
1038 [42] M. Stadler, M. Groissböck, G. Cardoso, A. Müller, and J. Lai, "Encouraging Combined
1039   Heat and Power in California Buildings," Ernest Orlando Lawrence Berkeley National
1040   Laboratory, Berkeley, California, USA, 2013.
1041 [43] "California Commercial End-Use Survey (CEUS)," California Energy Commission,
1042   Mar. 2006.
1043 [44] "Technology Characterization: Microturbines," Environmental Protection Agency -
1044   Climate Protection Partnership Division, Mar. 2002.
1045 [45] "Technology Characterization: Fuel Cells," Environmental Protection Agency -
1046   Combined Heat and Power Partnership Program, Dec. 2008.
1047

1048   **CVs**

1049

Christian Milan is currently pursuing the Ph.D. degree in thermal engineering from the Department of Energy Technology at Aalborg University, Denmark. He received the M.Sc. degree in 2010 in industrial engineering and management from the University of Flensburg, Germany. He spent a research internship at Berkeley Lab in 2013. His main research interests are focused on investment planning and operation of distributed energy systems, Net Zero Energy Buildings and residential supply systems
1057   based solely on renewable sources.

1058

Michael Stadler is a Research Scientist at Lawrence Berkeley National Laboratory, California, USA. He studied at Vienna University of Technology, from which he holds a Master's degree in electrical engineering and a Ph.D. summa cum laude in energy economics. He leads the microgrid and distributed energy resources group at Berkeley Lab and is the lead developer of DER-CAM. He is also the founder of the Center for Energy and innovative Technologies (CET) in Austria. Michael has published more than 160 papers, journal papers, reports, as well as five
1067   software tools in his 13 year career to date.

1068

Goncalo Cardoso is a Postdoctoral Fellow at the Lawrence Berkeley National Laboratory working for the Grid Integration Group of the Energy Storage and Distributed Resources Department. He received a M.Sc. in Civil Engineering from Instituto Superior Técnico, Technical University of Lisbon, Portugal, and later Ph.D. in Sustainable Energy Systems also from Instituto Superior Técnico within the MIT-Portugal Program. He focuses on Distributed Energy Resources Investment and Planning, having worked
1076   with DER-CAM since 2009, where he had several contributions including
1077   the implementation of stochastic capabilities, electric vehicle fleet modeling, critical loads,
1078   heat pumps, investment subsidies and feed-in tariffs within the California Self Generation
1079   Incentive Program, among others.
1080

1081

Salman Mashayekh is a Postdoctoral Fellow at the Lawrence Berkeley National Laboratory, Berkeley, CA, USA, working for the Grid Integration Group of the Energy Storage and Distributed Resources Department. He received his Electrical Power Systems B.Sc. and M.Sc. from University of Tehran, Iran, in 2006 and 2008, respectively, and his Ph.D. from Texas A&M University, College Station, TX, USA, in 2013. His research interests are in power and energy management methods in microgrids and buildings, electrical and cyber security in smartgrids, and applications of
1090   optimization in power and energy systems.

1091 **Figure captions**

1092 *Fig. 1. SANKEY diagram indicating energy flows in DER-CAM*

1093 ⇨ Intended for colour reproduction on the web
1094 ⇨ Intended for black-and-white in print
1095
1096
1097 *Fig. 2. Schematic representation of DER-CAM*

1098 ⇨ Intended for colour reproduction on the web
1099 ⇨ Intended for black-and-white in print
1100
1101 *Fig. 3. Maximal electrical efficiencies for natural gas powered ICEs*

1102 ⇨ Intended for colour reproduction on the web
1103 ⇨ Intended for black-and-white in print
1104

1105 *Fig. 4. Electrical efficiencies for a typical natural gas powered ICE in part load*

1106 ⇨ Intended for colour reproduction on the web
1107 ⇨ Intended for black-and-white in print
1108
1109 *Fig. 5. Schematic of the binary approach choosing efficiencies based on installed capacity*
1110 *and operational load level at each time step t*

1111 ⇨ Intended for colour reproduction on the web
1112 ⇨ Intended for black-and-white in print
1113
1114 *Fig. 6. Schematic of the approach based on SOS variable declarations to choose efficiencies*
1115 *changing with installed capacity and operational load level at each time step t*

1116 ⇨ Intended for colour reproduction on the web
1117 ⇨ Intended for black-and-white in print
1118

1119 *Fig. 7. Schematic of the implementation of the approach using SOS and binary variables into*
1120 *DER-CAM*

1121 ⇨ Intended for colour reproduction on the web
1122 ⇨ Intended for black-and-white in print
1123
1124 *Fig. 8. Electrical efficiencies for natural gas powered Micro Turbines*

1125 ⇨ Intended for colour reproduction on the web
1126 ⇨ Intended for black-and-white in print
1127
1128 *Fig. 9. Electrical efficiencies for natural gas powered Phosphoric Acid FC*

1129 ⇨ Intended for colour reproduction on the web
1130 ⇨ Intended for black-and-white in print
1131
1132 *Fig. 10. Accumulated optimal unit capacities for the four investigated buildings*

1133 ⇨ Intended for colour reproduction on the web
1134 ⇨ Intended for black-and-white in print
1135
1136 *Fig. 11. Accumulated hours of operation for all buildings at relevant load levels compared by*
1137 *applied modelling approach*

1138 ⇨ Intended for colour reproduction on the web
1139 ⇨ Intended for black-and-white in print